Int. J. Electrochem. Sci., 15 (**2020**) 4931 – 4943, doi: 10.20964/2020.06.11

International Journal of
ELECTROCHEMICAL
SCIENCE
www.electrochemsci.org

Short Communication

Bis-(3-sulfopropyl) Disulfide Acceleration of Copper Electrodeposition via Molecular Dynamics and Quantum Chemical Calculations

Fuliang Wang[1,2], *Yuping Le*[1,2,*]

[1] School of Mechanical and Electrical Engineering, Central South University, Changsha 410083, China
[2] State Key Laboratory of High Performance Complex Manufacturing, Changsha 410083, China
[*]E-mail: leyuping1@163.com

Received: 6 June 2019 / *Accepted:* 4 December 2019 / *Published:* 10 May 2020

Bis-(3-sulfopropyl) disulfide (SPS) is commonly used as an accelerator for copper electroplating in through-silicon via and printed circuit board fabrication. However, detailed SPS accelerator dynamics have not yet been fully studied. In this study, the adsorption behavior and accelerator dynamics of SPS on a copper surface were studied by using molecular dynamics and quantum chemical calculations. The natural atomic charges, molecular properties, distributions of frontier molecular orbitals, and Fukui indices were obtained. According to the simulations, the SPS reaction cycle on a copper seed layer surface was proposed. In this cycle, the SPS adsorbed on the cathode is attacked by H^+, Cl^-, and the oxygen anion of $-SO_3H$, obtains an electron from the cathode, and breaks into two 3-mercaptopropane-1-sulfonic acid (MPS) molecules. Subsequently, two free MPS dimerize into an SPS, releasing an electron to reduce Cu^{2+} into Cu^+. Through this SPS reaction cycle, electrons on the copper seed layer surface (cathode) are transferred to Cu^{2+} to yield Cu^+, thereby accelerating the deposition process.

Keywords: Bis-(3-sulfopropyl) disulfide, MD simulation, Quantum chemical calculations, HOMO, LUMO.

1. INTRODUCTION

Copper is the most commonly used interconnecting material in microelectronics, and copper electrodeposition is one of the most popular thin-film fabrication methods because of its simple operation, low cost, and high throughput [1-3]. Bis-(3-sulfopropyl) disulfide (SPS) [4, 5], in the form of a salt or an acid, is widely employed as an accelerator for copper electroplating methods such as dual-damascene electrodeposition, printed circuit board through-hole technology, and through-silicon

via (TSV) [6, 7] filling and has thus attracted significant research focus for several decades. One such system consisting of Cl^-, polyethylene glycol (PEG), SPS, and Janus Green B (JGB) was previously discussed by James [8]. For superfilling, PEG, SPS, and Cl^- must be present in the electroplating bath [9]. Superfilling was performed with 5 ppm JGB and 9 ppm SPS additives [10].

The interaction mechanism between SPS, Cl^- [11], and acid (H^+) is considered to be a key factor for high-performance copper electroplating solutions [12]. However, this complex interaction has not yet been completely elucidated. Hai et al. proposed a surface reaction cycle model to explain the behavior of SPS in damascene electrodeposition [13], and Broekmann et al. confirmed that SPS decomposes into 3-mercaptopropane-1-sulfonic acid (MPS) on the copper surface [14]. However, SPS adsorption to the surface and SPS separation into two MPS molecules have not been clearly explained.

The adsorption behavior of various molecules on a copper seed layer has been investigated through molecular dynamics (MD) simulations [15, 16], while molecular structures and chemical properties have been commonly analyzed by quantum chemical calculations [17-19]. Thus far, however, analyses of SPS acceleration properties by means of MD simulations and quantum chemical calculations have not been widely reported. In this study, the adsorption configuration, natural atomic charges, distributions of frontier molecular orbitals, and Fukui indices of SPS on a copper seed layer surface were explored in order to understand the acceleration mechanism, which offers a theoretical framework for the SPS acceleration principles. Finally, a novel SPS reaction cycle on a copper seed layer surface and the -S-S- bond breaking mechanism were proposed to explain how SPS can accelerate copper deposition.

2. COMPUTATIONAL SIMULATION DETAILS

Figure 1a shows SPS in an acidic environment, and Figure 1b shows bis-(3-sodiumsulfopropyl disulfide), or SPS in the form of a salt. Figure 1c shows the chemical structure of MPS in an acidic environment. In this simulation study, SPS and MPS were in the form of acids. SPS and MPS have been reported as excellent accelerators in many papers [4, 5, 11, 12, 20].

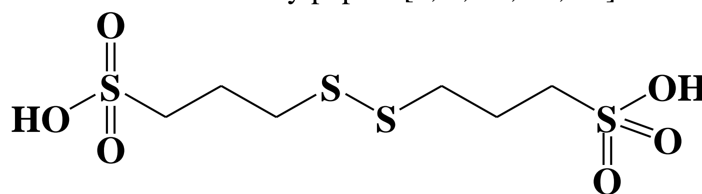

Bis-(sulfopropyl) disulfide acid
(a) SPS in acid solution

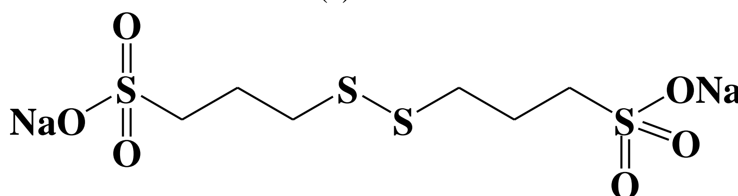

Bis-(3-sodiumsulfopropyl) disulfide
(b) SPS in salt form

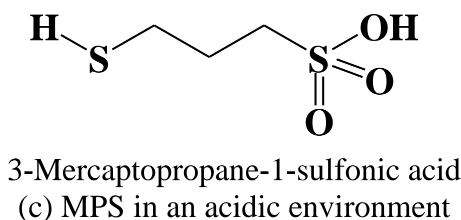

3-Mercaptopropane-1-sulfonic acid
(c) MPS in an acidic environment

Figure 1. Chemical structures of SPS and MPS.

2.1 MD simulation

The adsorption surface behavior of SPS molecules on a copper seed layer was investigated by MD simulations [21-23]. The simulations were performed in a box with periodic boundary conditions and dimensions of 2.0448 nm × 1.0224 nm × 3.5435 nm with repeated units representing the copper seed layer surface in Materials Studio software. These parameters allowed for a representative part of the interface to be modeled without arbitrary boundary effects. The simulation box consisted of a copper slab with a 2.5-nm-high vacuum layer on top. The crystals in the slab were cut along the (111) plane, keeping the uppermost and lowest layers free and the inner layer fixed. The simulation was carried out using an NVT/NVE ensemble, where the system atomic number (N), volume (V), and energy (E) remained unchanged. The simulation was carried out below 298 K, with the time step and simulation time set to 0.1 fs and 500 ps, respectively. The force field COMPASS was used for the entire simulation procedure.

The following equation was used to calculate the energy of SPS interacting with the copper surface ($E_{\mathrm{Cu\text{-}SPS}}$):

$$E_{Cu-SPS} = E_{complex} - E_{Cu} - E_{SPS}, \quad (1)$$

where E_{complex} is the total energy, and E_{Cu} and E_{SPS} are the total energies of the Cu crystal and free SPS, respectively.

2.2. Quantum chemistry calculations

Quantum chemical calculations [19, 24] were performed using GAUSSIAN 09W. The complete geometries of the additives were fully optimized without any symmetry constraints using B3LYP/6-31G (d, p) with GAUSSIAN 09W.

3. RESULTS

3.1 MD simulation

Since the adsorption characteristics of additives are intrinsically linked to their role in TSV filling, MD simulations were performed to study the adsorption behavior of SPS on a Cu (111) surface. As shown in Figure 2(a, b), the balanced temperature, potential energy, and non-bond energy indicate

that the system reaches equilibrium. The potential and non-bond energy decrease, illustrating that SPS adsorbed on the copper seed layer surface is more stable than the free SPS molecule.

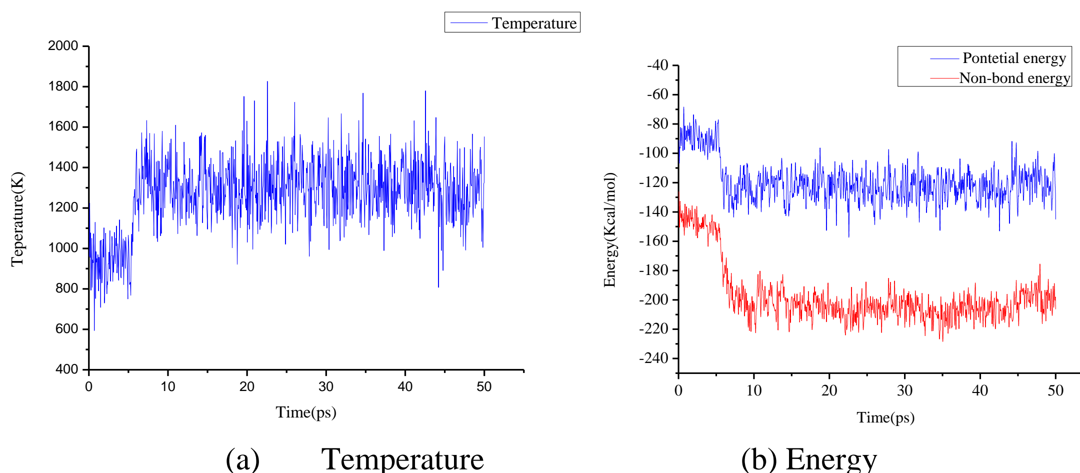

(a) Temperature (b) Energy

Figure 2. Temperature and energy of SPS molecule adsorbed on Cu (111) surface.

Figure 3(a, b) shows side views of an SPS molecule in the initial state and at equilibrium. All of the SPS atoms are adsorbed approximately parallel to the Cu surface at equilibrium, which shows that SPS can adsorb to the copper seed layer surface. The interaction binding energy of copper-SPS is -90.12 kJ/mol, while the binding energy is 90.12 kJ/mol, as listed in Table 1. These relatively small energies indicate that SPS easily adsorbs to and desorbs from the copper surface.

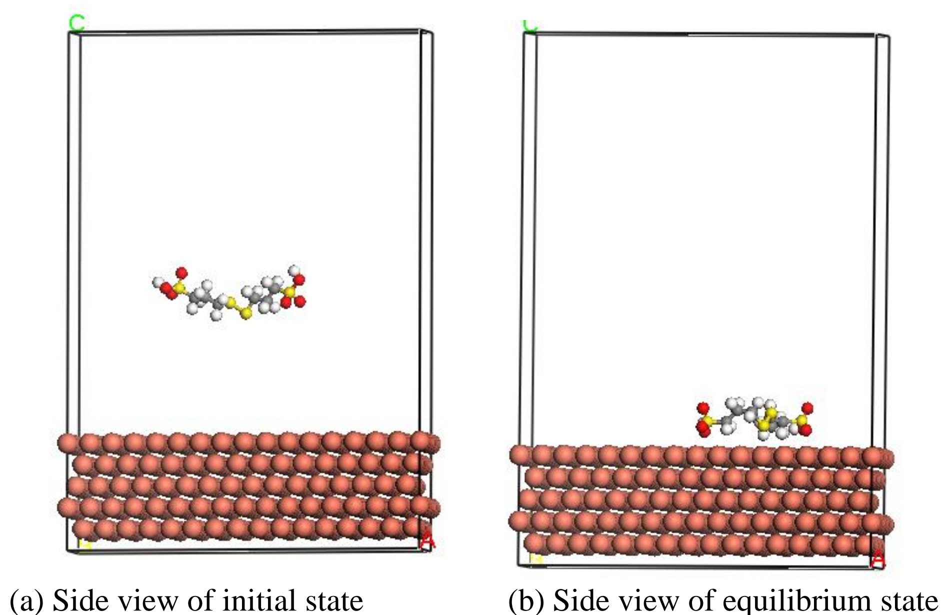

(a) Side view of initial state (b) Side view of equilibrium state

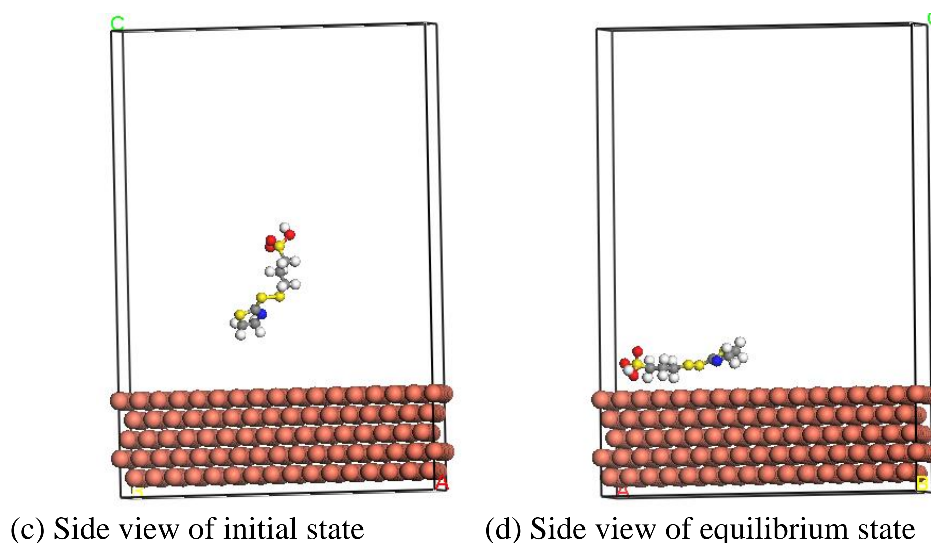

(c) Side view of initial state (d) Side view of equilibrium state

Figure 3. Configuration of SPS (a, b) and SH110 (c, d) molecules adsorbed on Cu (111) surface.

Table 1. Interaction and binding energy of SPS on Cu (111) surface

Accelerator	$E_{cu\text{-}accelerator}$ (kJ/mol)	$E_{binding}$ (kJ/mol)
SPS	-90.12	90.12

Based on the simulation, SPS is co-planarly adsorbed on the copper surface by the 3-mercaptopropanesulphonatein group at equilibrium. Initially, SPS is located away from the copper surface, and its shape resembles the letter "V." MD simulations were also performed to study the adsorption behavior of 3-(2-(4, 5-dihydrothiazol-2-yl)disulfanyl)propane-1-sulfonic acid or the sodium salt （SH110） on a Cu (111) surface, and the results are shown in Figure 3(c, d). SH110 is initially located far from the copper surface and is in the shape of the letter "V." The 4,5-dihydrothiazole groupwhich is Closer to the surface of the copper is below. The group of 3-mercaptopropanesulphonate which is Closer to the surface of the copper is above in the initial stage.

The acceleration afforded by SPS is superior to that afforded by SH110, which is an additive for acceleration and inhibition, as the thiazoline ring in thiazolinyl-S-Cu was approximately parallel to the copper surface according to the MD simulations [21, 22]. Thus, we conclude that SPS is an excellent additive since its atoms are adsorbed approximately parallel to the Cu surface at equilibrium.

3.2. Quantum chemistry calculations

We optimized the SPS spatial structure by the DFT B3LLP method in GAUSSIAN 09W. The optimized structure is shown in Figure 4. The atoms S1, S10, O1, O12, O13, O14, O15, and O16 are associated with -SO_3H, while S5 and S6 are within the -S-S- group. The relationship between structure and electrochemical behavior was investigated according to orbital information and electronic properties from SPS quantum chemical calculations. The natural atomic charges, molecular properties,

frontier molecular orbital distributions, and Fukui indices are considered to reveal the acceleration active sites of SPS.

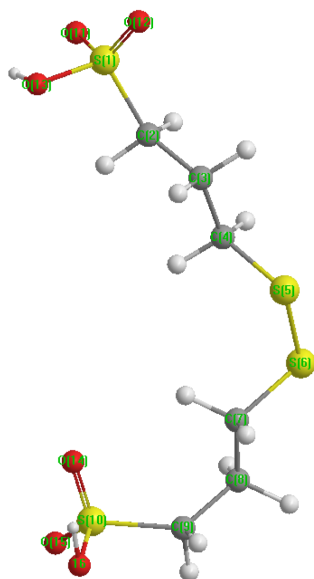

Figure 4. Optimized structure of SPS.

3.2.1 Natural atomic charges

The natural atomic charges of SPS on the Cu surface are given in Table 2. O11-O16 carry relatively large negative charges, which indicates that these atoms can supply electrons to the copper surface. S1 and S10 carry positive charges, which could result in bond feedback and strengthen the interaction between SPS and the copper seed layer. S1, S10, and O11-O16 are from $-SO_3H$, and thus $-SO_3H$ plays a major role in the chemical/physical adsorption of SPS to the Cu surface.

Table 2. Natural atomic charges of SPS

Atom	Charge	Atom	Charge
S1	0.546	C9	-0.21
C2	-0.208	S10	0.5409
C3	-0.156	O11	-0.325
C4	-0.177	O12	-0.291
S5	-0.076	O13	-0.305
S6	-0.089	O14	-0.313
C7	-0.166	O15	-0.286
C8	-0.150	O16	-0.315

3.2.2 Molecular property parameters

Based on Table 3, SPS has suitable electron donating (high E_{HOMO} at -0.2606 eV) and electron accepting (low E_{LUMO} at -0.2089 eV) capabilities. ΔE (E_{HOMO} - E_{LUMO}) is 0.0517 eV, indicating that SPS very easily interacts with other SPS molecules or other parts of itself. The interaction between the SPS molecules and Cu surface can be characterized by the total dipole moment (μ). The total dipole moment of SPS is as high as 6.419 D, suggesting that SPS interacts easily with the copper seed layer surface to form chemical/physical adsorption.

Table 3. Parameters of SPS properties

Parameter	Value
E_{HOMO} (eV)	-0.2606
E_{LUMO} (eV)	-0.2089
ΔE	0.0517
μ (D)	6.4199

3.2.3 Frontier molecular orbital distribution and Fukui indices

The orbital energy parameters of the SPS molecule are shown in Table 4. Orbital 81 is the HOMO (highest occupied molecular orbital), and orbitals 76-80 are the subordinate highest occupied molecular orbitals (NHOMOs). As the energy gaps between the NHOMOs and HOMO are as small as 0.02 eV, the NHOMOs and HOMO should all be considered in the study of the SPS reaction. Orbital 82 is the LUMO (lowest unoccupied molecular orbital), and orbitals 83-87 are the subordinate lowest unoccupied molecular orbitals (NLUMOs). The energy gaps between the NLUMOs and LUMO are as small as 0.07 eV, and thus the NLUMOs and LUMO should also be considered.

Table 4. Initial and equilibrium orbital energies of molecular SPS

Orbital	Energy (eV)	Orbital	Energy (eV)
76	-0.26760	82	-0.20892
77	-0.26680	83	-0.20431
78	-0.26649	84	-0.17976
79	-0.26602	85	-0.15738
80	-0.26237	86	-0.15400
81	-0.26061	87	-0.14085

The Fukui indices, which are the frontier electron densities normalized by the energy of the corresponding frontier molecular orbitals, are defined as

$$F_r^E = f_r^E / E_{HOMO}, \; F_r^N = f_r^N / E_{LUMO}, \quad (2)$$

where f_r^E is the electrophilic electron density of the donor molecule, f_r^N is the nucleophilic electron density of the acceptor molecule, F_r^E is the normalized f_r^E by E_{HOMO}, and F_r^N is the normalized f_r^N by E_{LUMO}.

Figure 5 and Table 5 show the initial NHOMOs and HOMO of SPS and their Fukui indices.

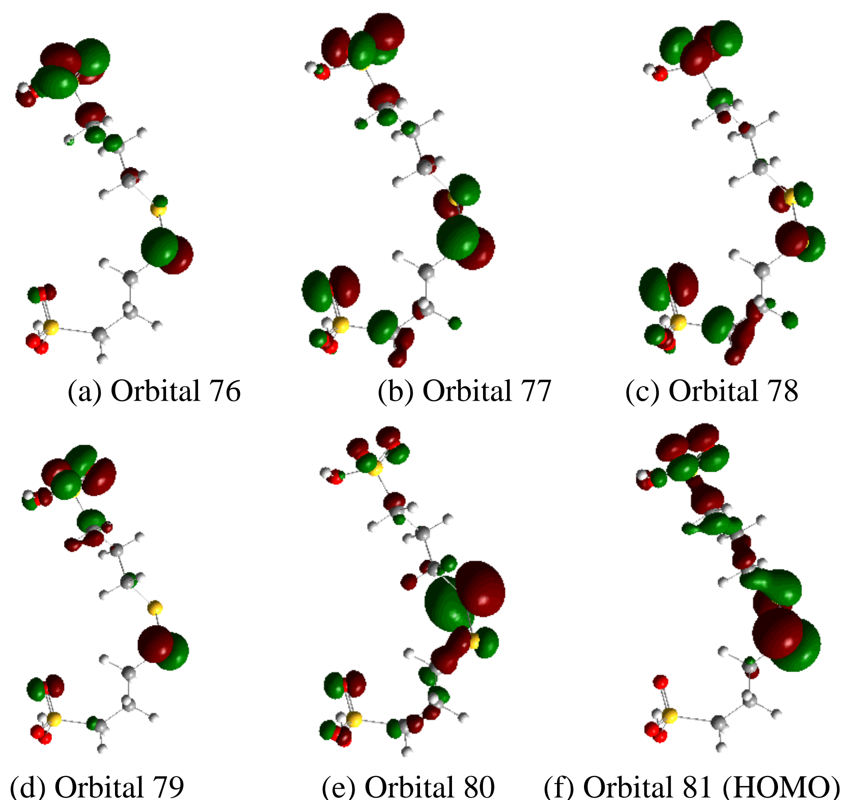

Figure 5. Geometry of SPS: (a-e) NHOMOs (76–80) and (f) HOMO (81).

Table 5. Fukui indices (F_r^E) and HOMO and NHOMO components (%) of SPS

Orbital / Atom	76		77		78		79		80		81	
	F_r^E	(%)	F_r^E	(%)	F_r^E	(%)	F_r^E	(%)	F_r^E	(%)	F_r^E	(%)
S1	-0.0288	1.12	-0.0070	0.27	-0.0031	0.12	-0.0128	0.49	-0.0032	0.11	-0.0202	0.74
C2	-0.1014	3.95	-0.0892	3.49	-0.0524	2.03	-0.1005	3.90	-0.0357	1.30	-0.1563	5.74
C3	-0.0192	0.75	-0.0114	0.45	-0.0093	0.36	-0.0049	0.19	-0.0054	0.19	-0.0335	1.23
C4	-0.0243	0.94	-0.0226	0.88	-0.0125	0.48	-0.0204	0.79	-0.0108	0.39	-0.0583	2.14
S5	-0.0229	0.89	-0.1144	4.48	-0.0610	2.36	-0.0050	0.19	-2.1241	77.70	-0.2931	10.76
S6	-0.2838	11.07	-0.3631	14.23	-0.1534	5.95	-0.3272	12.71	-0.1018	3.72	-1.3754	50.50
C7	-0.0011	0.04	-0.0034	0.13	-0.0034	0.13	-0.0015	0.05	-0.063	2.30	-0.0083	0.30
C8	-0.0009	0.03	-0.0155	0.60	-0.0227	0.88	-0.0024	0.09	-0.028	1.03	-0.0015	0.05
C9	-0.0044	0.17	-0.1318	5.16	-0.1991	7.73	-0.0169	0.66	-0.0322	1.17	-0.0015	0.05
S10	-0.0002	0.01	-0.0089	0.35	-0.0140	0.54	-0.0012	0.04	-0.0038	0.14	-0.0004	0.01
O11	-1.2312	48.04	-0.4496	17.62	-0.5436	21.10	-0.3222	12.52	-0.0536	1.96	-0.3136	11.51
O12	-0.7237	28.24	-0.5844	22.91	-0.3368	13.08	-1.5768	61.29	-0.0777	2.84	-0.3644	13.38
O13	-0.0654	2.55	-0.0091	0.36	-0.0073	0.28	-0.0444	1.72	-0.0072	0.26	-0.0403	1.48
O14	-0.0221	0.86	-0.6759	26.49	-1.0300	39.99	-0.0879	3.41	-0.1013	3.70	-0.0038	0.14
O15	-0.0008	0.03	-0.0258	1.01	-0.0432	1.67	-0.0044	0.17	-0.0353	1.29	-0.0039	0.14
O16	0	0	-0.0068	0.26	-0.0114	0.44	-0.0011	0.04	-0.0041	0.15	-0.0003	0.01
H (all)	-0.0312	1.22	-0.0313	1.23	-0.0715	2.77	-0.0422	1.64	-0.0456	1.66	-0.0481	1.76

According to Table 5, S6, O11, and O12 contribute to 87.35% of orbital 76, with O11 contributing the most; S6, O11, O12, and O14 contribute to 81.25% of orbital 77, with O14 contributing the most; S6, O11, O12, and O14 contribute to 80.12% of orbital 78, with O14 contributing the most; S6, O11, and O12 contribute to 86.52% of orbital 79, with O12 contributing the

most; S5 contributes to 77.70% of orbital 80; and S5, S6, O11, O12, and O13 contribute to 86.15% of orbital 81, with S6 contributing the most.

Because S1, S10, and O11-O16 are from -SO_3H, while S5 and S6 from -S-S- (as shown in Figure 4), the -SO_3H and -S-S- functional groups of SPS are the reaction centers of the molecule, from which electrons can be provided to other molecules, such as the copper surface and H^+. S5 in orbital 80 is the most reactive center, which could provide a negative charge based on frontier molecular orbital theory. In the solution for copper electroplating, hydrogen ions (H^+) are present on the copper surface, which can interact with -S-S-.

Figure 6 shows the LUMO and NLUMOs of SPS, and the main orbital components and F_r^N are listed in Table 6. The atoms C9, S10, O14, and O15, which are from CH_2-SO_3, contribute to 67.07% of orbital 82. S5 and S6, from -S-S-, contribute to 83.35% of orbital 84. Thus, it can be concluded that the -S-S- group is the most active site as it easily obtains a negative charge, and therefore it readily interacts with other molecules, such as chloride ions (Cl^-) and -SO_3H in the copper electroplating solution.

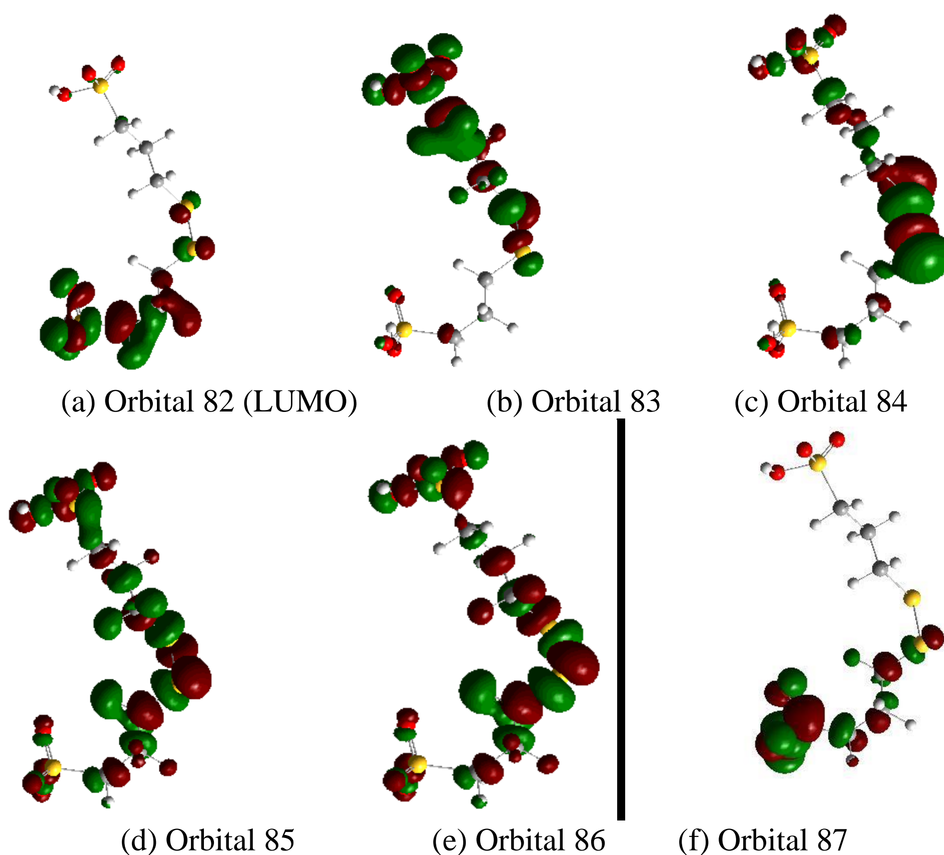

Figure 6. Geometry of SPS: (a) LUMO (82) and (b-f) NLUMOs (83–87).

Table 6. Fukui indices (F_r^N) and LUMO and NLUMO components (%) of SPS

Orbital / Atom	82		83		84		85		86		87	
	F_r^N	(%)	F_r^N	(%)	F_r^N	(%)	F_r^N	(%)	F_r^N	(%)	F_r^N	(%)
S1	-0.0087	0.21	-0.5057	11.47	-0.0924	1.82	-0.5259	7.68	-0.5042	6.69	-0.0037	0.05
C2	-0.0163	0.39	-0.9822	22.29	-0.1642	3.25	-0.1490	2.17	-0.1522	2.023	-0.0011	0.01
C3	-0.0085	0.20	-0.3616	8.20	-0.0746	1.47	-0.2931	4.28	-0.2995	3.97	-0.0006	0.00
C4	-0.0058	0.14	-0.3104	7.04	-0.0573	1.13	-0.7655	11.19	-0.7823	10.39	-0.0014	0.01
S5	-0.0649	1.57	-0.3873	8.79	-2.1137	41.84	-0.6569	9.60	-0.7239	9.61	-0.0036	0.05
S6	-0.1044	2.53	-0.1604	3.64	-2.0967	41.51	-0.8901	13.01	-1.3557	18.01	-0.1660	2.36
C7	0	0	-0.0012	0.02	-0.0358	0.71	-1.1142	16.28	-1.3297	17.66	-0.2645	3.76
C8	-0.3875	9.40	-0.0094	0.21	-0.0560	1.10	-0.3689	5.39	-0.3592	4.77	-0.1289	1.83
C9	-1.2162	29.52	-0.0338	0.76	-0.0572	1.13	-0.1919	2.80	-0.1745	2.319	-0.3709	5.27
S10	-0.5464	13.26	-0.0151	0.34	-0.0169	0.33	-0.0849	1.24	-0.1060	1.40	-2.8444	40.43
O11	0	0	-0.4551	10.32	-0.0477	0.94	-0.1483	2.16	-0.1300	1.727	-0.0008	0.01
O12	-0.0080	0.19	-0.4307	9.77	-0.0712	1.41	-0.2369	3.46	-0.1954	2.596	-0.0008	0.01
O13	-0.0060	0.14	-0.3631	8.24	-0.0953	1.88	-0.4604	6.73	-0.4028	5.353	-0.0020	0.02
O14	-0.4427	10.74	-0.0117	0.26	-0.0133	0.26	-0.0519	0.75	-0.0542	0.72	-0.4516	6.42
O15	-0.5584	13.55	-0.0142	0.32	-0.0133	0.26	-0.0532	0.77	-0.0586	0.77	-0.6700	9.52
O16	-0.32	7.79	-0.0088	0.20	-0.0105	0.20	-0.0602	0.88	-0.0756	1.00	-1.8896	26.86
H (all)	-0.4235	10.28	-0.3548	8.05	-0.0343	0.68	-0.7884	11.52	-0.8215	10.91	-0.2338	3.32

4. DISCUSSION

In the curvature enhanced accelerator coverage (CEAC) model reported by Josell et al. [25-29], mass conservation and relative adsorption strengths are the most important factors [28, 30]. However, there are essential drawbacks of CEAC, and it cannot explain why SPS acts as an accelerator. Yan et al. proposed a surface reaction cycle model to explain the behavior of SPS in damascene electrodeposition [12], and Hai et al. confirmed that SPS decomposes into MPS on the copper surface [13]. However, the underlying reasons for SPS adsorption to the surface and SPS separation into two MPS molecules have not been clearly explained.

According to the simulation results, a novel SPS reaction cycle model was proposed, as shown in Figure 7. The model can be considered to agree with both the CEAC [25-29] and adsorption models [31, 32]. The reaction cycle includes six steps.

Step 1: Two MPS molecules react with a Cu^{2+} to produce one SPS molecule. At the beginning of the cycle, two free MPS dimerize into an SPS when Cu^{2+} is present in the solution, and Cu^{2+} is reduced into Cu^{+} [13, 14]. Then, SPS physically adsorbs onto the Cu surface via the -S-S- or $-SO_3^-$ groups, as shown in Figure 3b. The -S-S- and $-SO_3^-$ groups have lone pair electrons (as shown in Tables 2 and 5 and Figure 5), which can be donated to the empty Cu orbital. Thus, these groups interact with the copper seed layer surface, resulting in a transformation from physical adsorption to chemical/physical adsorption.

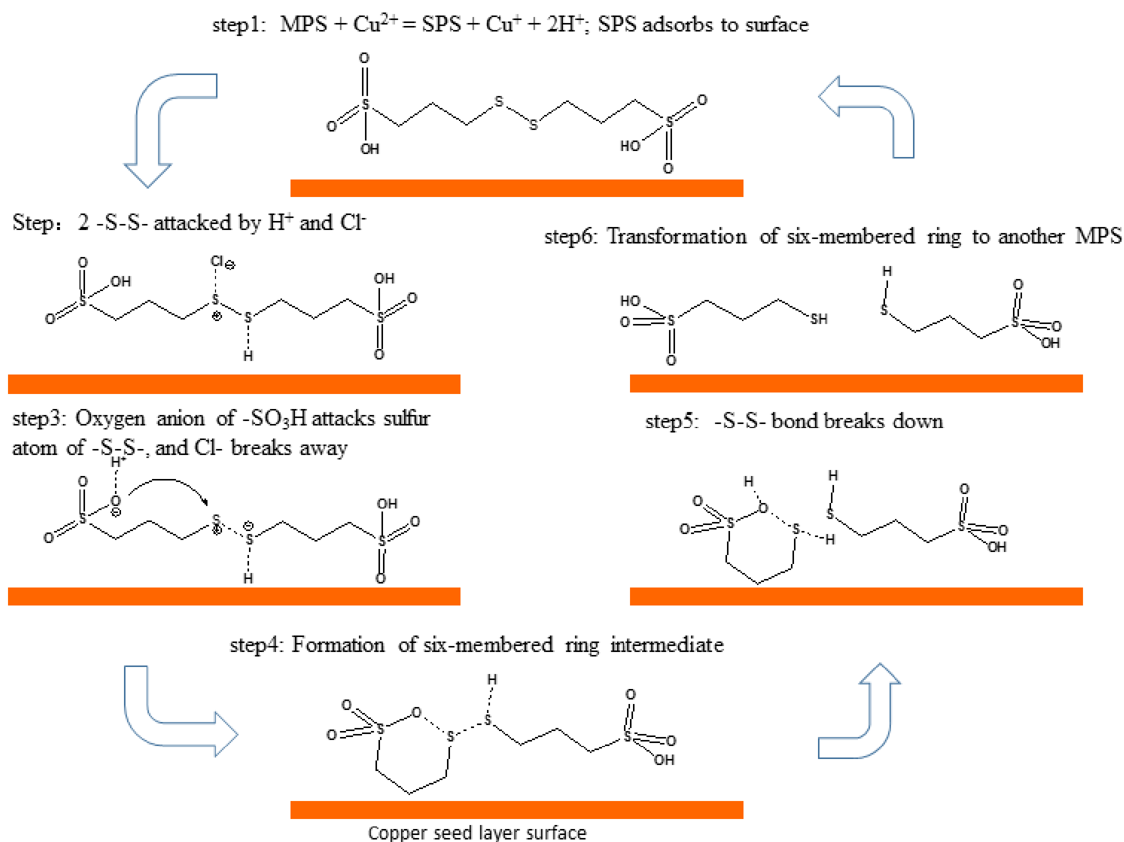

Figure 7. Schematic of SPS reaction cycle on copper seed layer surface

Cl^- concentration is the most important factor determining how SPS adsorbs to the copper surface. At high Cl^- concentrations, $-SO_3H$ points away from the copper surface. Thus, adsorption of SPS is more likely to occur by -S-S- [33]. At low Cl^- concentrations, physical adsorption occurs via both -S-S- and $-SO_3H$. However, chemical adsorption preferentially occurs via $-SO_3H$, as the oxygen atom of $-SO_3H$ has a higher electron density than that of -S-S- (as shown in Tables 2 and 5 and Figure 5), which results in the adsorbed molecules lying down on the copper surface (as shown in Figure 3). For TSV filling, the typical Cl^- concentration is as low as 10^{-6} mol/L; thus, SPS adsorbs onto the Cu seed surface via either -S-S- or $-SO_3^-$ (as shown in Figure 3b), preferentially via $-SO_3H$.

Step 2: H^+ and Cl^- attack the -S-S- group. After SPS adsorbs to the copper surface, -S-S- is first attacked by H^+, as electrons from -S-S- can be provided to other molecules (as shown in Figure 5 and Table 5). This changes -S-S- into an anion-cation pairing, allowing for the sulfide attacked by H^+ to become the most active site, which easily obtains a negative charge. Then, Cl^- attacks the other sulfide atom of -S-S-, since -S-S- as an active site easily obtains a negative charge based on the LUMO and NLUMOs (as shown in Figure 6 and Table 6).

Steps 3-4: The oxygen anion of $-SO_3H$ attacks the sulfur atom of -S-S- that was attacked by Cl^-, as it has a partial positive charge. This leads to the formation of a six-membered ring intermediate, because the six-membered ring is the most stable ring in organic chemistry. The synergistic action of chloride and SPS has been reported by Broekmann et al. [14].

Step 5: With the help of $2H^+$, SPS is broken down to one MPS molecule and a six-membered ring. At the same time, SPS obtains an electron from the copper surface in the electroplating process. This is treated as the most important step for the acceleration of TSV copper filling.

Step 6: The six-membered ring intermediate is unstable and becomes another MPS molecule. The two free MPS molecules are then ready for the next cycle. MPS and H_2O-Cu(I)-MPS would be formed under the condition of SPS as an additive.

Therefore, this SPS reaction cycle can transfer an electron from the copper seed layer surface (cathode) to Cu^{2+} to yield Cu^+ and accelerate the deposition process. The accelerating property of SPS can only be realized by the SPS molecule being broken into two free MPS molecules on the cathode surface in the presence of electrons, Cl^-, and H^+ since SPS and MPS are interconvertible. Hai et al. in fact proved that SPS would be the product of intermediate MPS [13].

5. CONCLUSIONS

The adsorption behavior of an SPS molecule on a copper seed layer surface was investigated by MD simulations, which showed that SPS adsorbs parallel to the Cu surface. The calculated Fukui indices show that the $-SO_3H$ and -S-S- functional groups of SPS are the reaction centers, and that electrons from the two centers can be provided to other molecules such as the copper surface and H^+, Cl^-, and $-SO_3H$ in the copper electroplating solution.

According to quantum chemical simulations, the SPS reaction cycle on the copper seed layer surface was proposed as follows. a) SPS physically adsorbs on the Cu surface via -S-S- or $-SO_3^-$ and gives electrons to an empty Cu orbital, changing the physical adsorption to chemical/physical adsorption. b) Then, H^+ and Cl^- attack the -S-S- group, and the oxygen anion of $-SO_3H$ attacks the sulfur atom of -S-S- attacked by Cl^-, which forms a six-membered ring intermediate. c) Next, with the help of $2H^+$, SPS is broken down to one MPS molecule and a six-membered ring; at the same time, SPS obtains an electron from the copper surface during the electroplating process. d) Finally, the unstable six-membered ring becomes another MPS molecule. The two free MPS molecules dimerize into an SPS, releasing an electron to reduce Cu^{2+} into Cu^+. Through this SPS reaction cycle, electrons from the copper seed layer surface (cathode) can be transferred to Cu^{2+} to yield Cu^+, which accelerates the deposition process.

ACKNOWLEDGMENTS
The authors are thankful for the project support from the China Department of Science & Technology Program 973 (Contract No.: 2015CB057202).

References

1. J. Reid, *Jpn. J. Appl. Phys.,* 40 (2001) 2650.
2. M. A. Pasquale, L. M. Gassa and A. J. Arvia, *Electrochim. Acta*, 53 (2008) 5891.
3. Z. Y. Jian, T. Y. Chang, Y. C. Yang, W. P. Dow, S. L. Yau and Y. L. Lee, *Langmuir*, 25 (2009) 179.
4. Z. Y. Jian, T. Y. Chang, Y. C. Yang, W. P. Dow, S. L. Yau and Y. L. Lee, *Langmuir*, 25 (2009) 179.

5. W. P. Dow, M. Y. Yen, C. W. Liu and C. C. Huang, *Electrochim. Acta*, 53 (2008) 3610.
6. M. Motoyosh, *Proc. IEEE*, 97 (2009) 43.
7. J. H. Lau, *Microelectron. Int*., 28 (2011) 8.
8. J. J. Kellya and A. C. West, *Electrochem. Solid-State Lett.*, 2 (1999) 561.
9. W. P. Dow, H. S. Huang and Z. Lin, *Electrochem. Solid-State Lett.*, 6 (2003) C134.
10. Y. Cao, P. Taephaisitphongse, R. Chalupa and A. C. West, *J. Electrochem. Soc.*, 48 (2001) C466.
11. Y. F. Liu, Y. L. Lee, Y. C. Yang, Z. Y. Jian, W. P. Dow and S. L. Yau, *Langmuir*, 26 (2010) 13263.
12. J. J. Yan, L. C. Chang, C. W. Lu and W. P. Dow, *Electrochim. Acta*, 109 (2013) 1.
13. N. T. M. Hai, T. T. M. Huynh, A. Fluegel, M. Arnold, D. Mayer, W. Reckien, T. Bredow and P. Broekmann, *Electrochim. Acta*, 70 (2012) 286.
14. P. Broekmann, A. Fluegel, C. Emnet, M. Arnold, C. Roeger-Goepfert, A. Wagner, N. T. M. Hai and D. Mayer, *Electrochim. Acta*, 54 (2011) 4724.
15. S. Xia, M. Qiu, L. Yu, F. Liu and H. Zhao, *Corros. Sci.*, 50 (2008) 2021.
16. A. Kornherr, S. Hansal, W. E. Hansal, J. O. Besenhard, H. Kronberger, G. E. Nauer and G. Zifferer, *J. Chem. Phys*., 119 (2003) 9719.
17. C. J. Cramer and D. G. Truhlar, *Phys. Chem. Chem. Phys*., 11 (2009) 10757.
18. C. E. White, J. L. Provis, T. Proffen, D. P. Riley and J. S. Van Deventer, *Phys. Chem. Chem. Phys*., 12 (2010) 3239.
19. T. Lovell, F. Himo, W. G. Han and L. Noodleman, *Coord. Chem. Rev*., 238–239 (2003) 211.
20. S. E. Bae and A. A. Gewirth, *Langmuir*, 22 (2006) 10315.
21. C. Wang, J. Q. Zhang, P. X. Yang and M. An, *Int. J. Electrochem. Sci*., 7 (2012) 10644.
22. C. Wang, M. An, P. Yang and J. Zhang, *Electrochem. Commun*., 18 (2012) 104.
23. H. L. Tu, P. Y. Yen, S. Chen, S. L. Yau, W. P. Dow and Y. L. Lee, *Langmuir*, 27 (2011) 6801.
24. M. Karelson, V. S. Lobanov and A. R. Katritzky, *Chem. Rev*., 96 (1996) 1027.
25. T. P. Moffat, D. Wheeler, W. H. Huber and D. Josell, *Electrochem. Solid-State Lett.*, 4 (2001) C26.
26. A. C. West, S. Mayer and J. Reid, *Electrochem. Solid-State Lett.*, 4 (2001) C50.
27. T. P. Moffat, D. Wheeler, S. K. Kim and D. Josell, *Electrochim. Acta*, 53 (2007) 145.
28. T. P. Moffat, D. Wheeler, M. D. Edelstein and D. Josell, *IBM J. Res. Dev.*, 49 (2005) 19.
29. D. Wheeler, D. Josell and T. P. Moffat, *J. Electrochem. Soc.*, 150 (2003) C302.
30. D. Josell, T. P. Moffat and D. Wheeler, *J. Electrochem. Soc.*, 154 (2007) D208.
31. R. Akolkar and U. Landau, *J. Electrochem. Soc.*, 151 (2004) C702.
32. R. Akolkar and U. Landau, *J. Electrochem. Soc.*, 156 (2009) D351.
33. N. T. M. Hai. K. W. Kramer, A. Fluegel, M. Arnold, D. Mayer and P. Broekmann, *Electrochim. Acta*., 83 (2012) 367.

© 2020 The Authors. Published by ESG (www.electrochemsci.org). This article is an open access article distributed under the terms and conditions of the Creative Commons Attribution license (http://creativecommons.org/licenses/by/4.0/).